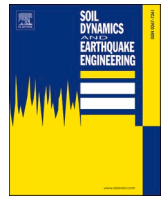




ELSEVIER

Contents lists available at ScienceDirect

Soil Dynamics and Earthquake Engineering

journal homepage: www.elsevier.com/locate/soildyn

Fines content determination through geotechnical and geophysical tests for liquefaction assessment in the Emilia alluvial plain (Ferrara, Italy)

Francesco Di Buccio^{a,*}, Cesare Comina^b, Daniela Fontana^c, Luca Minarelli^d, Federico Vagnon^e, Sara Amoroso^{a,d}

^a Dipartimento di Ingegneria e Geologia, Università degli Studi G. d'Annunzio di Chieti-Pescara, Pescara, Italy

^b Dipartimento di Scienze della Terra, Università degli Studi di Torino, Torino, Italy

^c Dipartimento di Scienze Chimiche e Geologiche, Università degli Studi di Modena e Reggio Emilia, Modena, Italy

^d Istituto Nazionale di Geofisica and Vulcanologia, Sezione Roma1, L'Aquila, Italy

^e Dipartimento di Ingegneria dell'Ambiente, del Territorio e delle Infrastrutture, Politecnico di Torino, Torino, Italy

ARTICLE INFO

Keywords:

Fines content
Liquefaction assessment
Geophysical tests
Cone penetration test
Flat dilatometer test

ABSTRACT

The influence of the fines content on the cyclic resistance has been widely studied and the importance of the determination of this parameter from different geotechnical tests has been underlined for liquefaction assessments. Geotechnical evidences from local investigations may however not completely reflect the lateral subsoil variability, which is important for the identification of localized potential liquefaction phenomena. Geophysical tests can be useful in the imaging of these lateral variations and related fines content variability. In this study calibration of existing fines content correlations with piezocone tests are accomplished and new specific correlations are proposed to assess the fines content both from flat dilatometer and geophysical tests in two liquefied research sites of the Emilia alluvial plain (Italy), following the 2012 earthquakes. The proposed correlations are tested in a third site showing the usefulness of the fines content determination for liquefaction assessment, and its imaging in 1D and 2D profiles.

Author statement

Di Buccio F: Writing, Software, Formal analysis, Data curation, Reviewing and Editing, Investigation.

Comina C: Conceptualization, Methodology, Writing - Original Draft preparation, Investigation.

Fontana D: Conceptualization, Reviewing and Editing, Investigation.

Minarelli L: Conceptualization, Validation, Data curation, Investigation.

Vagnon F: Software, Formal analysis, Data curation, Investigation.

Amoroso S: Conceptualization, Methodology, Writing - Original Draft preparation, Investigation.

1. Introduction

During the latest decades several procedures for liquefaction assessment have been developed (e.g. Refs. [1–10]). These procedures are based on geotechnical and geophysical in-situ tests, such as Standard Penetration Test (SPT), Cone Penetration Test (CPT), Flat Dilatometer

Test (DMT), Chinese Dynamic Cone Penetration Test (DPT) and shear wave velocity measurements (V_S). SPT, CPT and V_S procedures already foresee the application of a correction factor for the fines content (FC) of the soils susceptible to liquefaction. However, as observed [11], the fines content correction applied to the normalized in-situ test parameters using a “blind” FC estimate or a laboratory-calibrated FC relationship provides high differences into the susceptibility evaluation (e.g. thickness and depth of the liquefied layer, classification of the site according to the available severity liquefaction indexes, agreement between liquefaction prediction and liquefaction observations). Therefore, accurate liquefaction analyses require site-specific FC estimates representative of the regional geological framework which influences the soil properties of a specific area.

The FC determination on site is usually non trivial, since it can be performed following detailed sampling and grain-size analyses, even though this approach does not provide continuous FC profiles and is significantly expensive and time consuming. Alternatively, the FC can be estimated by means of empirical correlations with resistance parameters from geotechnical tests. The soil behaviour type index (I_c), obtainable

* Corresponding author.

E-mail address: francesco.dibuccio@unich.it (F. Di Buccio).

<https://doi.org/10.1016/j.soildyn.2023.108057>

Received 23 December 2022; Received in revised form 25 May 2023; Accepted 25 May 2023

Available online 9 June 2023

0267-7261/© 2023 The Authors. Published by Elsevier Ltd. This is an open access article under the CC BY license (<http://creativecommons.org/licenses/by/4.0/>).

from CPT tip resistance (q_c) and sleeve friction (f_s), can be for example used. The I_c parameter is somehow correlated with FC and commonly used in liquefaction assessments (e.g. Refs. [7,12]). However, there is considerable scatter in the data on which the FC- I_c correlations are based (e.g. Refs. [13–15]). Boulanger and Idriss [7] attributed the large scatter observed within each dataset to three main factors; (1) lateral and vertical geologic variability occurring over very short distances; (2) fundamental limitations in the I_c parameter when attempting to categorise a wide group of soil types and (3) uncertainty associated with the influence of soil plasticity. As the I_c parameter is based on correlations with the mechanical behaviour of soils, and due to inherent soil variability, it is crucial to develop site-specific correlations and fitting parameters, which can be adjusted to calibrate the empirical FC- I_c equations to peculiar site conditions (based on laboratory testing).

Similar shortcomings can be associated to other in-situ tests, such as the flat dilatometer test (DMT), for which it is possible to estimate soil types using the material index (I_D) according to Marchetti and Crapps [16]. As for the I_c , the I_D is not a grain-size distribution index, but it reflects the mechanical response of the soil deposits (e.g. Ref. [17]) supplementing also to discern free-draining from non-free-draining layers [18]. However, no specific FC-DMT correlations are yet available in the international literature. Geotechnical evidences from the abovementioned punctual investigations may not identify the lateral subsoil variability, which is important for the identification of localized potential liquefaction phenomena (e.g. Ref. [19]). In this respect, geophysical tests could be crucial for imaging the lateral variations and for a more comprehensive view of the geological variability at the study site. Recent studies (e.g. Refs. [20–22]) suggested the use of combined geophysical measurements of electrical resistivity (R) and shear wave velocity (V_s) for a direct FC determination through appropriate mixture theories. Goff et al. [23] proposed a new relationship between soil type, R and V_s . Hayashi et al. [24] developed a second order multivariable polynomial equation from a least squares regression fit of cross-plotted R and V_s data to distinguish clays, sands, and gravels. Recently, Takahashi et al. [22] proposed a method for profiling the clay content from R and V_s data by implementing the unconsolidated sand model and the Glover's model [25]. A similar approach has been adopted by Vagnon et al. [26,27] for obtaining 2D FC sections from combined R and V_s measurements along river embankments and earth dams.

In this paper both geotechnical (CPT and DMT) and geophysical tests (based on R and V_s) in the Emilia plain (Ferrara province, Italy) are studied in the aim of developing reliable FC determinations of the specific study area, strongly affected by liquefaction phenomena following the 2012 seismic sequence [28]. Specific correlations at two trial test sites are compared with laboratory evidences from borehole samples. Particularly, a new devoted correlation is proposed to derive FC from DMT and analysis of existing approaches to determine FC from geophysical data are evaluated. The established correlations are then used to image the FC variability in a third test site both along 1D profiles and 2D sections. In developing the proposed procedure this study took advantage of the rich dataset and accurate geological, geotechnical and geophysical knowledge available in the Emilia plain [15]. The combined geotechnical and geophysical approach may be particularly effective in reconstructing the subsoil configuration of alluvial settings, characterized by high lateral and vertical variability in sediment type and grain-size. In particular, the FC imaging may allow to identify the upper non-liquefiable high FC crust covering the lower FC liquefiable layers, representing a pivotal contribution in reliable liquefaction assessment.

2. Geological setting

The study area is part of the Po plain basin, the syntectonic sedimentary wedge filling the Pliocene–Pleistocene Apennine foredeep. The structural setting of the Po basin originated in response to the collision between the Adria microplate and Eurasia during the Cenozoic. High subsidence rates due to the tectonic loading, associated with strong

sediment input, generated a thick Pliocene–Quaternary succession [29]. The basin infill is up to 4 km-thick, and the Quaternary deposits reach a thickness of 1.5 km.

The study area within the Ferrara plain (Fig. 1) corresponds to the buried frontal portion of the compressive ramp, and the associated active faults are responsible of the well documented seismic activity [30] which in several cases has induced critical liquefaction phenomena (red dots in Fig. 1), as for the Emilia seismic sequence in 2012 [28].

The main drainage, the Po River, interacts with a dense network of transverse tributaries. The river network continuously shifted laterally as a consequence of climate changes and local tectonic events [31]. The late evolution of the alluvial system has been traced following the physical evidence of paleochannels on the alluvial plain surface [32], and the provenance composition of buried channel sands compared with present day rivers [33,34].

The engineering geological map (Fig. 1) was derived from the critical synthesis of the available seismic microzonation studies, using the geological-technical units defined by SM Working Group (2015) in agreement with Unified Soil Classification System USCS [35]. This map describes the surface distribution of the fluvial sediments deposited by the Po and by some Apennine rivers, such as Reno and Panaro. The study sediments largely consist of mostly inorganic lean clays (CL, according to the USCS [35]), deposited into moist inter-river depressions. The argillaceous units are crisscrossed by sinuous silty sandy bodies (SM, according to USCS classification), deposited into fluvial channels, and potentially subjected to liquefaction phenomena. The Po sandy bodies are generally coarser and less silty than the Apennine bodies [15]. The channel bodies are often flanked by levee deposits, by fluvial crevasse splays, or by the granular infilling of minor river channels (silt and sandy silts, ML, according to USCS classification).

All the studied sites are characterized by an argillaceous crust, cohesive and not liquefiable, with a variable thickness ranging from 3 m in the northern site of Bondeno (Fig. 1b) to 6 m in Mirabello (Fig. 1a) and up to 9 m in the southernmost site of San Carlo (Fig. 1c) [36,37]. The argillaceous crust overlies liquefiable buried silty sands and sandy silts (SM, ML) organized in vertically stacked channel-belt bodies referable to the Po River (Bondeno, Mirabello) or as thin, relatively narrow lens-shaped bodies of silty sands and sandy silts with an Apennine signature, deposited by the Reno River (San Carlo site).

Within this geological context, the geotechnical and geophysical characterization is mainly focused: 1) to provide an estimate of the thickness of the shallower high FC portion of the subsoil, which corresponds to the non-liquefiable crust (increased thickness of the crust will result in reduced liquefaction hazard), and 2) to estimate the FC in the underlying sandy silt and silty sand layers to evidence zones more prone to liquefaction (increased FC in these layer will result in reduced liquefaction hazard).

3. Methodologies for the fines content estimation

3.1. FC estimates from geotechnical in-situ tests

Site-specific calibrations using laboratory tests are required to provide reliable FC estimations through correlations with resistance parameters from geotechnical tests, otherwise parametric analyses are recommended to evaluate the sensitivity to FC estimates (e.g. Ref. [7]). In this study, the equations proposed by Suzuki et al. [38] (Eq. (1)) and Boulanger and Idriss [7] (Eq. (2)) as a function of the soil behaviour type index (I_c) from CPT:

$$FC = x_c \cdot (2.8 \cdot I_c^{2.6}) \quad (1)$$

$$FC = 80 \cdot (I_c + C_{FC}) - 137 \quad (2)$$

were applied and calibrated using available direct geotechnical investigations (grain-size analyses on borehole samples).

Both the equations include a correlation coefficient, x_c for Suzuki

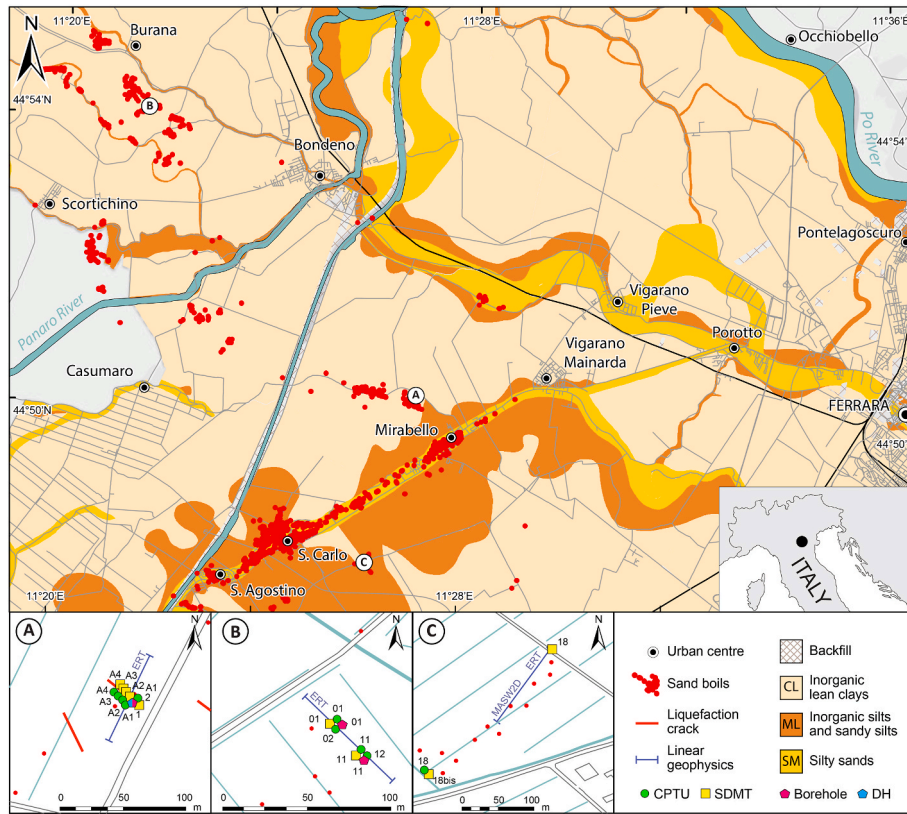


Fig. 1. Engineering geological map of the outcropping alluvial deposits of the studied area within the Emilia plain in the Ferrara province (Italy) with evidence of the liquefaction phenomena referable to the Emilia seismic sequence in 2012 (red dots); in (a), (b) and (c) details of the studied sites (Mirabello, Bondeno and San Carlo, respectively) and executed geotechnical and geophysical tests are reported.

et al. [38] and C_{FC} for Boulanger and Idriss [7], which takes into account the variability of the datasets used by the authors. The range of variability of these coefficients is quite wide and, as suggested by the authors, is site-specific. In particular, x_c ranges between 0.5 and 2, while C_{FC} varies from a minimum value of -0.29 to a maximum of 0.29 . The variability of these coefficients has been therefore analysed for two test sites (Fig. 1a-b) within the 2012 Emilia earthquake epicentral area and calibrated to obtain site-specific FC-correlations with CPT. Moreover, the first fines content correlation starting from DMT results has been proposed. The proposed FC-DMT equation involves, similarly to CPT, the I_D parameter and a calibration coefficient to consider the variability of the dataset, which has been obtained from a linear regression using flat dilatometer and laboratory data of the studied sites.

3.2. FC estimates from geophysical tests

The conceptual workflow adopted for the evaluation of FC from geophysical tests is reported in Fig. 2. The workflow is based on the construction of theoretical R and V_s curves as a function of FC to which associate the observed experimental data.

In detail.

a) the Glover's equation ([25]) is adopted to exploit the relationship between soil porosity (Φ) and resistivity (R) considering also the degree of saturation as in the following:

$$\frac{1}{R} = \frac{1}{R_g} \cdot (1 - \phi)^{\frac{\log(1-\phi^m)}{\log(1-\phi)}} + \frac{1}{R_f} \cdot \phi^m \cdot S_w^q \quad (3)$$

where R is the overall resistivity of the soil, R_g and R_f are respectively the soil grain and fluid resistivities, m is the cementation factor, q is the saturation index and S_w is the saturation degree.

b) the Hashin-Shtrikman upper bound model [39] is adopted to express R_g as a function of the constituting grains (mixture of sand and silt/clay):

$$\frac{1}{R_g} = \frac{1}{R_{clay}} \left[1 - \frac{3 \cdot (1 - FC) \cdot \Delta R}{\frac{3}{R_{clay}} - FC \cdot \Delta R} \right] \quad (4)$$

where FC is the fines content, R_{clay} is the clay resistivity and ΔR is defined as:

$$\Delta R = \frac{1}{R_{clay}} - \frac{1}{R_{sand}} \quad (5)$$

where R_{sand} is the resistivity of non-clay particles.

c) Hashin-Shtrikman lower bound [39] and the Voigt-Reuss-Hill model [40] are adopted to infer the relationship between soil porosity (Φ) and shear wave velocity (V_s), using the following equations:

$$V_s = \sqrt{\frac{\left(\left(\frac{\phi}{G_{HM} + Z} + \frac{1 - \phi}{G_g + Z} \right)^{-1} - Z \right)}{\rho}} \quad (6)$$

with:

$$Z = \frac{G_{HM} \cdot 9 \cdot K_{HM} + 8 \cdot G_{HM}}{6 \cdot K_{HM} + 2 \cdot G_{HM}} \quad (7)$$

$$K_{HM} = \left[\frac{n^2 \cdot (1 - \phi)^2 \cdot G_g^2 \cdot P}{18 \cdot \pi^2 \cdot (1 - \nu)^2} \right]^{\frac{1}{3}} \quad (8)$$

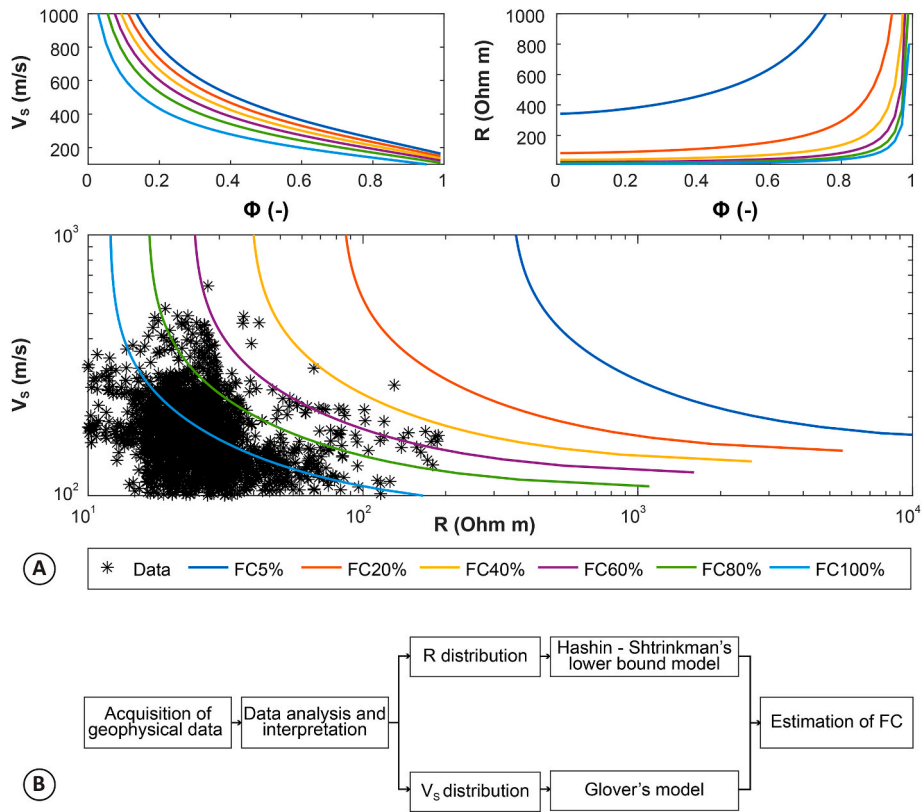


Fig. 2. (a) Theoretical V_s - Φ , R - Φ and V_s - R relationship as a function of theoretical FC for a given depth and superimposed example distribution of field data. (b) Workflow for estimating FC using multiple geophysical data (modified from Vagnon et al. [27]).

$$G_{HM} = \left[\frac{5 - 4 \cdot \nu}{5 \cdot (2 - \nu)} \right] \cdot \left[\frac{3 \cdot n^2 \cdot (1 - \phi)^2 \cdot G_g^2 \cdot P}{2 \cdot \pi^2 \cdot (1 - \nu)^2} \right]^{\frac{1}{2}} \quad (9)$$

$$G_g = \left[\frac{(1 - FC) \cdot G_{sand} + C \cdot G_{clay} + \left(\frac{1 - FC}{G_{sand}} + \frac{FC}{G_{clay}} \right)^{-1}}{2} \right] \quad (10)$$

where ρ is the bulk density of the soil, G_{HM} and K_{HM} are respectively the shear and bulk moduli of the soil at the critical porosity, Φ_0 , n is the coordination number, P is the confining pressure, ν is the Poisson's ratio of the soil, G_{sand} and G_{clay} are respectively the shear moduli of sand and silt/clay components, and G_g is the shear modulus of the soil grains.

All the constitutive parameters of the above equations can be obtained by in-situ geological and geotechnical information or assumed based on the wide scientific literature on this topic (such as R_{clay} and R_{sand}). Further details about the choice of the constitutive parameters and on the sensitivity analysis of the above equations can be found in Vagnon et al. [27].

By superimposing the measured R and V_s values at a given depth to the theoretical constant FC curves, it is then possible to obtain the soil FC associating the experimental data to the nearest FC curve. Specific calibrations are also possible if direct FC estimations are available at a particular site to compare the results. This approach has been attempted in this study changing the constitutive parameters to allow the better possible match with available direct geotechnical investigations at the two calibration sites (Fig. 1a-b).

4. Geotechnical and geophysical characterization at the calibration sites and site-specific FC estimates

The sites adopted for the calibration of the proposed procedure refer to Mirabello (Fig. 1a) and Bondeno (Fig. 1b), two villages located in the

province of Ferrara (Italy), strongly affected by liquefaction phenomena following the 2012 Emilia seismic sequence. These sites have been studied through numerous research activities, including full-scale blast-induced liquefaction experiments, to which the data used in this work refer. In particular, the Mirabello test site (Fig. 1a) was the site of the first Italian blast-induced liquefaction test performed in silty sands. Its main goal was to study the variation of soil properties before and after the execution of the blast test sequence [19,36], by performing piezocone (CPTU), seismic dilatometer (SDMT), down-hole tests (DH) in boreholes, and electrical resistivity tomographies (ERT). On the contrary, the Bondeno test site (Fig. 1b) was realized to study the effectiveness of rammed aggregate piers towards liquefaction mitigation in silty sands using explosives, and geotechnical and geophysical tests (boreholes, CPTU, SDMT, ERT) were performed before and after treatment, and after the blast at different times [9,11,37].

The subsoil model of the Mirabello test site can be identified using the available borehole log and related laboratory tests, the DH and ERT surveys, five CPTUs and five SDMTs performed along a 2012 liquefaction crack (see Fig. 1). The schematic soil profile with the USCS classification is reported in the first line of Fig. 3 together with the FC data obtained from laboratory tests [34] and the in-situ soil type indicators, the I_c from CPTU and the I_p from DMT. Direct measurements from the site investigations are also reported in the second line of Fig. 3 in terms of the corrected cone resistance (q_p) from CPTU, the horizontal stress index (K_D) from DMT, the shear wave velocity (V_s) from DH, and the resistivity (R) from ERT.

The measurements highlight a thick non-liquefiable crust in the upper 6 m, characterized by silts and clays, CH-CL according to USCS classification, with fines content $FC \approx 70$ –100% and plasticity index $PI \approx 23$ –54%. The underlying layers are mainly composed by low plastic non plastic sandy silts and silty sands of Apennine (Reno River) provenance, litharenitic in composition, (ML-SM with $FC \approx 25$ –75%, $PI \approx 5$ –9% between 6 and 8 m depth) and quartz-feldspar-rich Alpine (Po

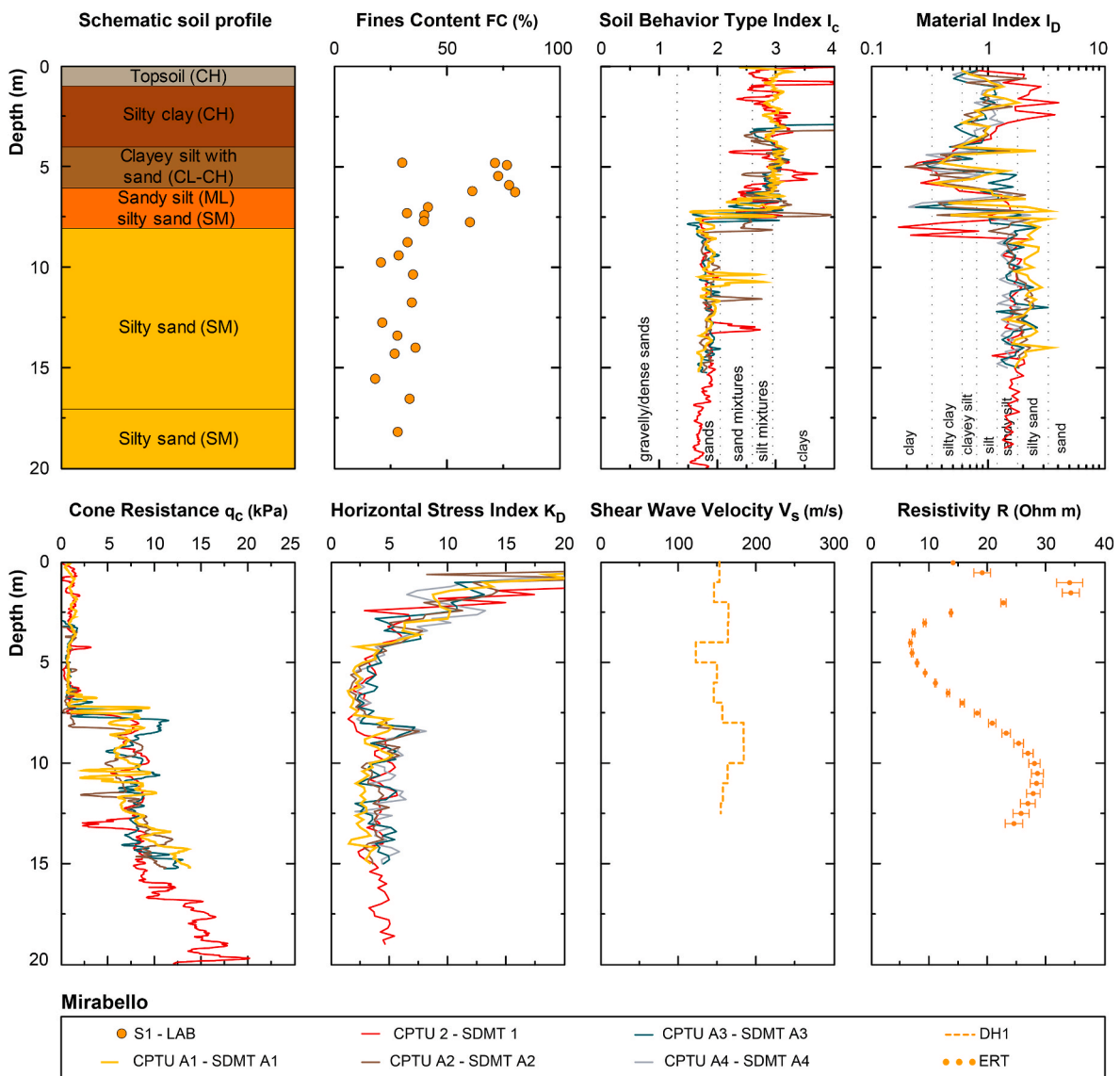


Fig. 3. Soil profiles at the Mirabello test site. First line: schematic soil profile with USCS classification, fines content (FC) from laboratory tests, soil behaviour type index (I_c) from CPTU, material index (I_D) from DMT; second line: corrected cone resistance (q_c) from CPTU, horizontal stress index (K_D) from DMT, shear wave velocity (V_s) from DH, resistivity (R) from ERT.

River) provenances (SM with $FC \approx 20\text{--}35\%$, $PI \approx 0\%$, below 8 m depth). Fontana et al. [34] identified the litharenitic silty sands with Apennine provenance as the source layer that liquefied in 2012, by comparing compositional and grain-size analyses on the borehole samples and the sand boils. This assessment matches well with the CPT and DMT profiles: q_t values are limited approximately between 0.8 and 2 MPa and K_D data varies from about 1.5 to 3 in the Apennine-derived layer, while both the parameters have a considerable increase in the deeper Alpine-derived sand layers ($q_t \approx 6\text{--}18$ MPa, $K_D \approx 3\text{--}6$).

Coherently with the above results the DH test identifies a first silty clay layer (V_s of about 150 m/s) 3 m thick. Below this layer, a velocity inversion is observed in the clayey silty layer from 4 to 6 m (V_s of about 120 m/s). Thereafter, a progressive increase in V_s in the Apennine sandy silts and silty sands and in the underlying Po sandy loams is observed. DH data were obtained at the site by means of a seismic chain of 8 triaxial (10 Hz) geophones with 1 m spacing, connected to a Geonics-Geode seismograph. The seismic chain was lowered into the hole with a 2 geophones superposition for consecutive lowerings. For the acquisitions a 5 kg sledge-hammer striking laterally on a 1.5 m steel bar was adopted. Source polarity inversion was also used. Data were processed,

after first break picking, both with the interpolation method and with the true interval method following the ASTM D7400-14 [41] standards and in ISSMGE guidelines [42]. Good quality data were obtained in most acquisitions (for more details see Ref. [19]) allowing a very reliable soil profile reconstruction.

The V_s results are confirmed by the ERT results. A shallow resistive (resistivity of about 30 Ohm·m) layer (topsoil and silty clays) 4 m-thick is observed. This layer corresponds to the high-velocity layer identified by the DH test and is related to the presence of a dry crust at the time of execution of the tests, due to an arid winter season. A less resistive (resistivity of about 7 Ohm·m) layer is observed from 4 to 6 m, related to the presence of saturated clayey silts. A noticeable increase in resistivity is observed between 6 and 8 m in the fluvial Apennine deposits, while the resistivity results approximately constant in the Po River silty sands. ERT data were acquired with a Syscal-Pro georesistivitymeter and 72 electrodes at 1 m spacing. A Wenner-Schlumberger acquisition sequence was adopted with 1287 potential measurements. This sequence allowed a dense spatial distribution of measuring points combining both lateral and vertical resolution (for more details see Ref. [19]). Experimental data were inverted with Res2DInv [43] after filtering of anomalous

measurements (with standard deviations higher than 5%). A very good convergence of the results was obtained from the inverted resistivity model with a global root mean square error below 2%. The resistivity profile reported in Fig. 3 was then obtained from the inverted resistivity model by considering the average resistivity with depth in the zone (within a 1 m radius) where the other geotechnical data were available (see Fig. 1a). Variability from the average resistivity value span from 7%, near the surface to 1–2% at depth, averaging 3.35%. The relatively higher variability near surface reflects the more laterally heterogeneous top soil.

At the Bondeno test site the geotechnical model was reconstructed using the two available borehole logs and the related laboratory tests, four CPTUs, two SDMTs and the ERT. The location of the surveys is reported in Fig. 1 and covers a wide area, extended about 70 m and largely affected by the 2012 sand ejecta. The summary of the geotechnical and geophysical characterization is reported in Fig. 4. The reconstructed stratigraphic column is composed by a thin silty-clayey non-liquefiable crust in the upper 3.5 m depth, namely CL for USCS classification, with FC > 65% and PI ≈ 18–22%, followed by a non-plastic thick sandy and silty-sandy layer with considerable values of FC ≈ 25–35% (SM-SP). According to the liquefaction assessment presented by

Amoroso et al. [11] using the “simplified method” [1], the 2012 liquefied deposits can be detected into the upper layer of Po River silty sands (depth approximately between 3.5 and 12 m), characterized by lower values of resistance and stiffness. However, as highlighted already by the authors, the fines content correction applied to the CPT procedure using a “blind” FC estimate or a laboratory-calibrated FC relationship provides high differences into the susceptibility evaluation, resulting important to provide a site-specific FC estimate for the 2012 Emilia epicentral area.

Geophysical evidences are in good agreement with geotechnical tests. Results of the SDMT test identify a first silty-clayey layer (V_s around 100 m/s) about 3–4 m thick. Below this layer, a progressive velocity increase is observed in the thick sandy and silty-sandy layer (V_s from 150 to 250 m/s). SDMT data were obtained at the site with two horizontal geophones (frequency of 28 Hz and sensitivity of 0.600 V/ips), spaced 0.5 m, for measuring V_s each 0.5 m [44]. A biaxial inclinometer is also located at the midpoint of the seismic probe to monitor the tilt during the penetration and to eventually correct V_s measurements. A manual hammer hitting horizontally an appropriate base is used to generate S-waves at the ground surface. The S-wave source, 10 kg heavy, is oriented parallel to the receiver axis to increase the sensitivity to the generated shear waves. The S-wave source, connected to a

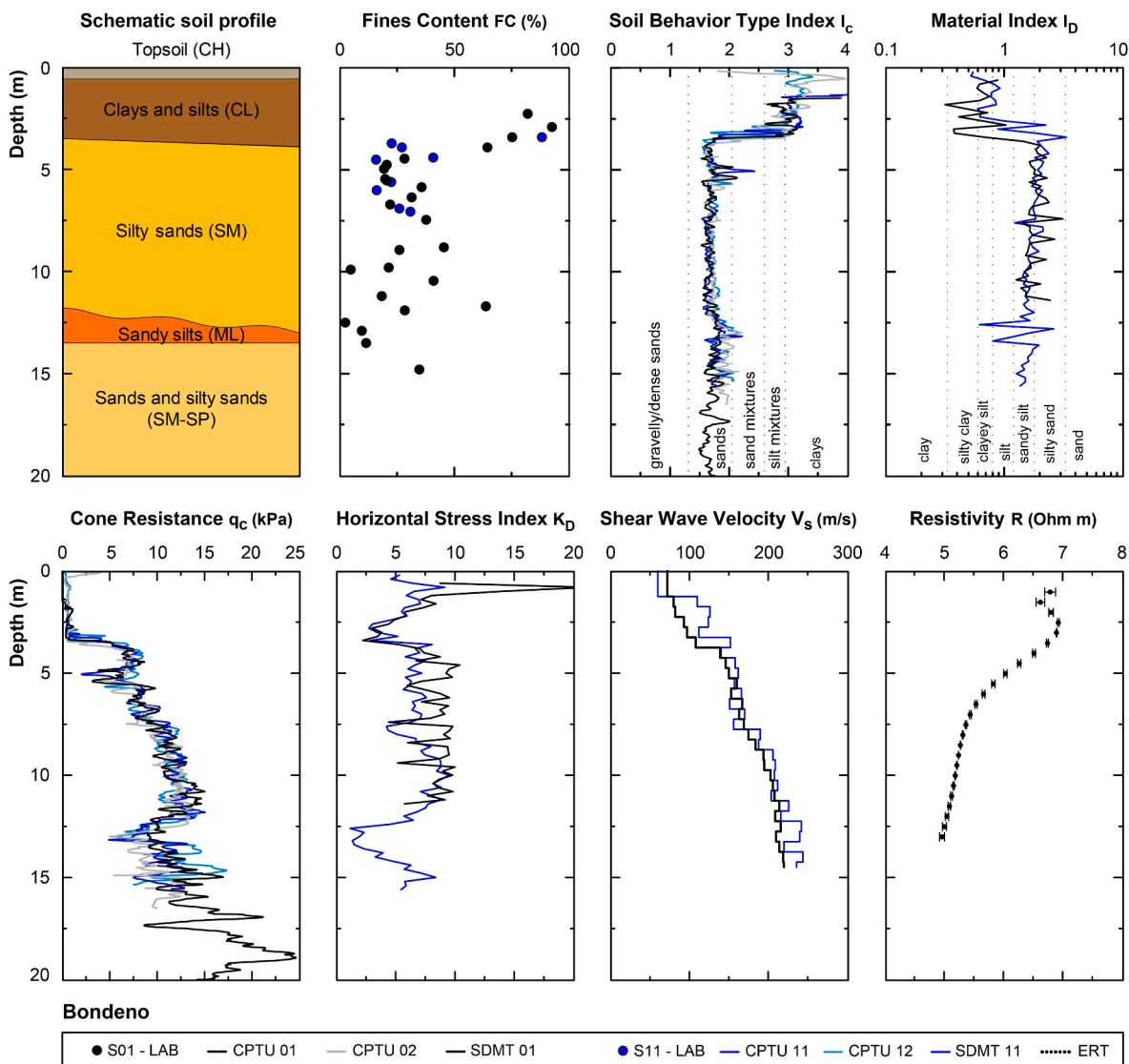


Fig. 4. Soil profiles at the Bondeno test site. First line: schematic soil profile with USCS classification, fines content (FC) from laboratory tests, soil behaviour type index (I_c) from CPTU, material index (I_D) from DMT; second line: corrected cone resistance (q_c) from CPTU, horizontal stress index (K_D) from DMT, shear wave velocity (V_s) from SDMT, resistivity (R) from ERT.

different external trigger, is usually located at a distance of less than 1 m from the DMT penetrating rods to have the S-waves travel nearly vertical. The seismic signal, acquired by the geophones, is amplified and digitized at depth. The recording system consists of one channel for each geophone, having identical phase characteristics and adjustable gain control. Usual sampling interval of 200 μ s is used for S-waves. A similar processing approach than for the DH data was adopted allowing good quality data and a very reliable soil profile reconstruction.

Generally, very low resistivities were measured at the test site due to anomalous very high electrical conductivity of the saturating water (above 1300 μ S/cm). These high conductivity values strongly influenced the imaged resistivity data towards lower resistivity values, partially compromising the ability of the surveys in detecting stratigraphic changes. Nevertheless, a clear transition is evidenced in the resistivity profile from the silty-clayey layer in the upper 3.5 m depth (resistivity of about 7 Ω m) to the following sandy and silty-sandy layers (resistivity of about 5 Ω m). ERT data were acquired with a Syscal-Pro georesistivitymeter and 64 electrodes at 1 m spacing. A similar Wenner-Schlumberger acquisition sequence than in the Mirabello site was adopted with 990 potential measurements, reduced with respect to Mirabello due to the reduced array length. Data were inverted with the same approach than in the Mirabello site with an even increased convergence (global root mean square error below 1%). As before the resistivity profile reported in Fig. 4 was then obtained from the inverted resistivity model considering the average resistivity with depth in the zone (within a 1 m radius) where the other geotechnical data were available (see Fig. 1b). Variability from the average resistivity value span in this case from 1.3% near the surface to about 0.05% at depth, averaging 0.45%. The relatively low variability, reduced with respect to the Mirabello site, reflects the high fluid conductivity that tend to homogenize the whole resistivity section.

4.1. Calibration of FC estimates

The x_c (Eq. (1) [38]) and C_{FC} (Eq. (2) [7]) coefficients have been calibrated using the FC values obtained by laboratory tests and the available CPTU data at the Mirabello and Bondeno test sites. In order to obtain a single I_c value to associate to the laboratory FC, I_c was averaged at ± 0.1 m with respect to the depth of the analysed sample. The plot of the entire I_c -FC dataset shows a high variability of the C_{FC} values mostly in the 0.00 to 0.40 range and in the 1 to 4 range for the x_c coefficient, as reported in Fig. 5a-b. The best fitting of the C_{FC} and x_c values (red curves in Fig. 5a-b) reports a positive value of $C_{FC} = 0.19$ for Boulanger and Idriss [7] and the upper bound of the Suzuki et al. [38] formulation equal to $x_c = 2$.

The availability of flat dilatometer data have allowed to propose the

first correlation between the material index (I_D) and the fines content. During the DMT soundings, the measurements were collected every 0.2 m, therefore the I_D was averaged at ± 0.2 m with respect to the sample depth. The coupling of the DMT and laboratory data has provided the following linear regression (red line in Fig. 5c):

$$FC = x_D \cdot (-31 \cdot I_D + 91) \tag{11}$$

Upper and lower bounds in the correlation can be detected using a coefficient named x_D that varies from 0.5 to 2 (dashed lines in Fig. 5c). Furthermore, in all the plots of Fig. 5, dot vertical lines have been added according to the soil type thresholds identified by I_c and I_D , which may be useful in additional refinements of calibration for indirect FC estimates obtained in further investigations in these areas.

The application of the calibrated coefficients to single CPTU and DMT at the research sites allowed to compare the site-specific FC predictions with the FC laboratory measurements. Analogously to geotechnical tests, the procedure described in Section 3.2 was used for forecasting FC from geophysical surveys.

Fig. 6 plots the FC estimates by CPTU and DMT for the Mirabello and Bondeno test sites, together with the FC estimates from the geophysical tests and available laboratory data. The indirect FC estimates (from geotechnical and geophysical tests) are reasonably in good agreement with the laboratory FC data points. For both the sites the sharp vertical variations between clays/silts and silty sands, at about 6 m at the Mirabello site and 3 m at the Bondeno site, are satisfactorily reproduced by all the adopted indirect methodologies. Results based on the geophysical tests at the Mirabello test site appear to show a shallower thickness of the clay layer apparently in accordance with some laboratory FC estimates. Both the DMT and geophysical estimates appear to show a reduced FC in the upper portion of the cohesive crust where laboratory data are limited. Within the underlying sandy silt/silty sand layers, the proposed correlations show a greater variability which is also displayed in the laboratory FC estimates. Particularly at the Bondeno site results based on the geophysical tests seem to diverge from the ones from the geotechnical tests below about 6 m depth. This behaviour can be related to the higher subsoil variability (laboratory FC varying between 10 and 50% below 5 m depth) and therefore to the more localized nature of geotechnical testing with respect to the geophysical ones. Indeed, also the different estimates from geotechnical testing are less in agreement in this test site. However, this effect can be also partially related to the high fluid conductivity at the Bondeno test site which can partially drive the geophysical estimates to higher FC.

Regarding CPT predictions, the assumed Sukuki et al. [38] coefficient ($x_c = 2$) provides a FC profile that fits better to the laboratory data than using the site-specific Boulanger and Idriss [7] coefficient ($C_{FC} = 0.19$). This is also confirmed by comparing the overall standard

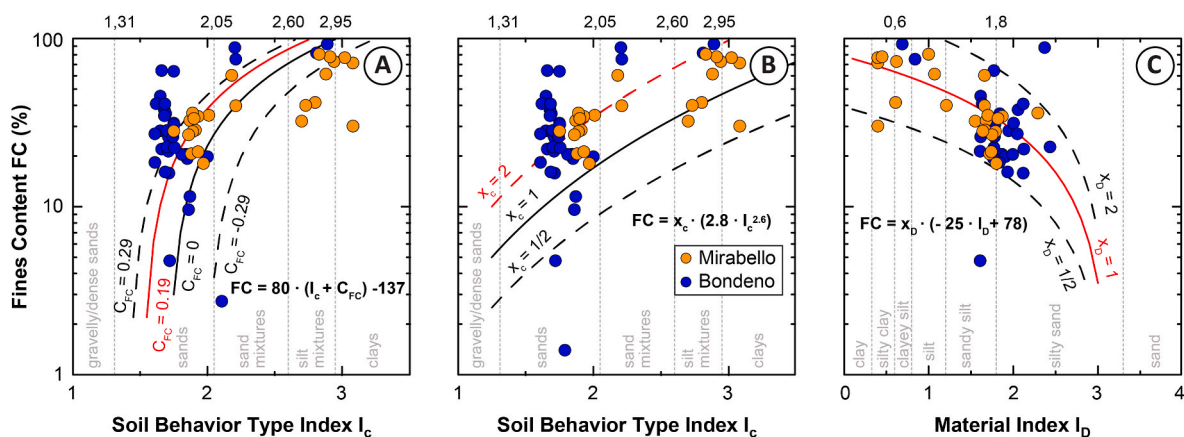


Fig. 5. FC estimates using in-situ tests at the Mirabello and Bondeno test sites: (a) calibration of the I_c -FC chart by Ref. [7]. (b) Calibration of the I_c -FC chart by Ref. [38]. (c) I_D -FC chart proposed in this study based on DMT data.

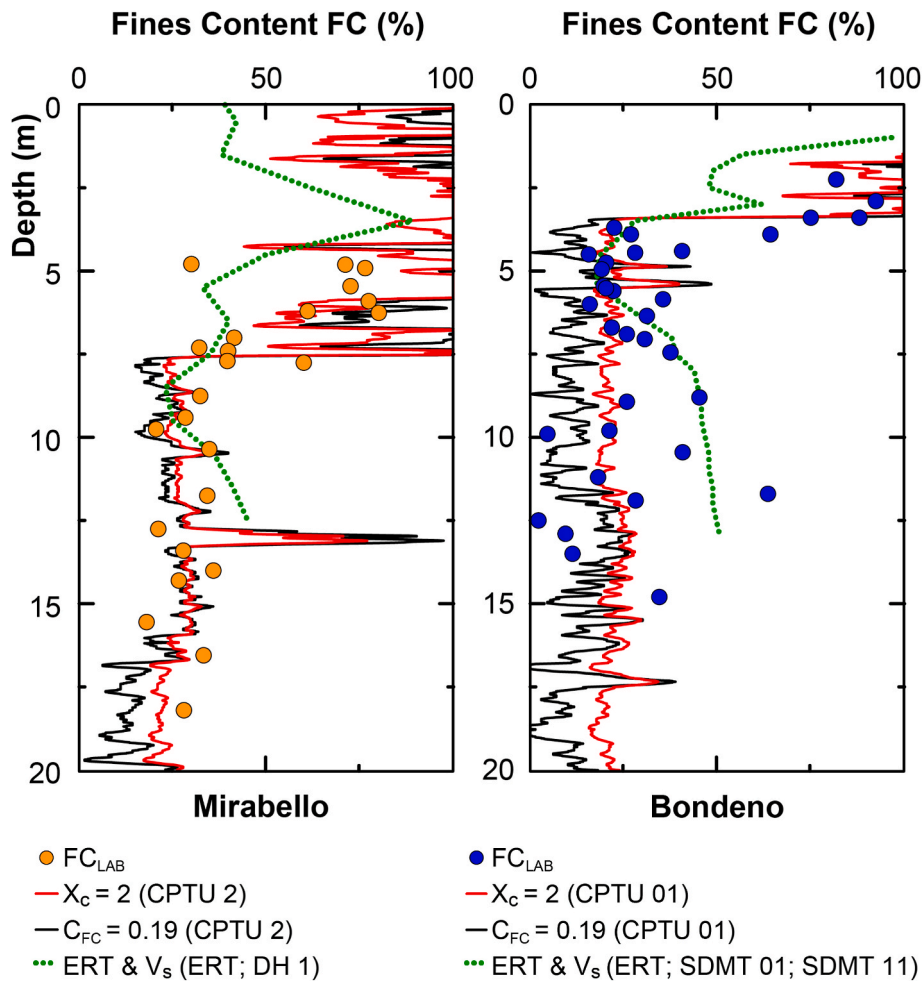


Fig. 6. Comparison between FC profiles at the Mirabello and Bondeno test sites: laboratory data (FC LAB), estimates using CPT relationships with $x_c = 2$ [38] and $C_{FC} = 0.19$ [7], new FC predictions by DMT and geophysical surveys (ERT and V_s from DH or SDMT).

deviation (SD) of the FC predictions with respect to the laboratory measurements:

$$SD = \frac{\sqrt{\sum (FC_{CPT} - FC_{LAB})^2}}{N} \quad (12)$$

where FC_{CPT} is the FC prediction obtained by CPT correlations, FC_{LAB} is the FC value measured in the laboratory and N the total number of measurements. At both the test sites, the SD based on the Suzuki et al. [38] estimate (25% in Mirabello and 17% in Bondeno) is lower than that the one obtained using the Boulanger and Idriss [7] equation (31% in Mirabello and 21% in Bondeno) allowing an overall better agreement with the laboratory data.

The comparison between the FC measurements and predictions from the newly proposed DMT correlation (Fig. 5) seems to perform better in the silty sandy layer, where the number of laboratory samples is considerably higher, compared to the upper cohesive crusts (few available samples). The average SD for the DMT correlation is 23% in Mirabello and 24% in Bondeno, therefore of the same order of the CPT correlations.

The FC profile estimated from geophysical surveys is also in reasonably good agreement with laboratory measurements, highlighting the potentialities of the proposed methodology for a preliminary screening of the potentially liquefiable soil and upper cohesive crust. The average SD for the geophysical correlation at both the sites is 32% in Mirabello and 22% in Bondeno.

5. Application of the calibrated correlations at the San Carlo test site

The correlations described in the previous sections have been used to forecast the FC variability in the third site of San Carlo (Fig. 1c) both along 1D profiles (geotechnical correlations) and 2D sections (geophysical correlation). As shown in Fig. 1, both ERT and MASW2D surveys were performed along the direction where the 2012 sand boils occurred at the site, while two SDMTs and one CPTU were carried out at the border of the same alignment.

Both the geophysical surveys have the same length (106.5 m) and acquisition spacing (electrodes and geophones 1.5 m-spaced) to guarantee a perfect overlap of the results and good compromise between the depth of investigation (DOI) and the data coverage. ERT data at this site were obtained following similar approaches than in the calibration sites. Particularly the same approach adopted at the Mirabello site was used for data acquisition (Syscal-Pro georesistivitymeter and 72 electrodes at 1 m spacing with same Wenner-Schlumberger acquisition sequence with 1287 quadrupole). Also data processing and inversion was similar with a very good convergence (global root mean square error below 1%). As already mentioned this sequence allowed a dense spatial distribution of measuring points combining both lateral and vertical resolution with a resulting resolution of about 0.5 m both in the vertical and horizontal direction.

The seismic data were instead analysed with a specific procedure for the analysis of Rayleigh wave fundamental mode dispersion curves [45, 46] to allow the reconstruction of a 2D V_s section. This approach is

based on the use of a direct Wavelength-Depth transform of experimental dispersion curves and does not require a formal solution of the inverse problem. This transform has been obtained considering the similitude between the weighted average V_S profile and the dispersion curve and represents the surface waves skin depth for increasing wavelengths. Further detail on the way in which this transform was obtained and can be applied for 2D V_S section reconstruction can be found in Anjom et al. [47]. In this same paper a study on the uncertainty analysis of this approach was also reported showing that minor and uniform uncertainties (less than 10% in most regions) can be obtained.

Using the calibrated methodologies described in sections 3 and 4, the 2D imaging of FC for the San Carlo test site has been evaluated from the geophysical data and the 1D FC profiles obtained from available geotechnical tests (Fig. 8). The colour scale adopted for the FC representation is similar to the one used for the stratigraphic profiles of the calibration sites (see Figs. 3 and 4) to allow a direct comparison.

ERT results (Fig. 7a) are in good agreement with the attended stratigraphic scheme in the area reporting: a shallow layer of topsoil with quite high resistivity (ranging between 60 and 100 Ohm•m) which can be related to the extremely arid conditions during the measurements, till the depth of 2 m; below a more conductive layer (resistivity lower than 10 Ohm•m) of clays and silts, with a variable thickness of 4–7 m and a resistive layer (ranging between 20 and 30 Ohm•m) of sandy silts. Within this last layer local increases in resistivity are imaged reflecting the local presence of silty sands. The interface between the clayey and sandy silt/silty sand deposits is not horizontal but exhibits elongated resistivity anomalies, which might be correlated with liquefaction effects occurred during the 2012 earthquake. It must be however considered that due to the presence of the low resistivity clay layer a reduction in sensitivity is observed in the final inverted model below about 7 m depth. This effect still allows to consider very reliable the imaging of the interface between the clayey and sandy silt/silty sand deposits but less certain the resistivity values below this interface.

A similar setting emerges from the seismic tests at the site (Fig. 7b). Below a shallow low-velocity (V_S lower than 100 m/s) layer of clays and silts, a progressive increase in V_S is observed, due to the passage to sandy silts and silty sands. This last transition is better evidenced in the seismic data with respect to the resistivity data which conversely have higher resolution in the identification of the shallow topsoil. Similarly to the ERT section the transition from clayey and sandy silt/silty sand deposits is not horizontal but exhibits localized anomalies in which portions of soil with V_S values up to 120 m/s are mixed (particularly at 45 and 80 m progressives) in a more homogeneous clayey layer with average V_S lower than 100 m/s. In particular, at 80 m progressive, it is clearly visible the material uplift up to the surface potentially correlated to the observed liquefaction phenomena in the same portion of the profile (see Fig. 1).

From these results it can be observed that, even if the punctual 1D tests are not in the same position of the 2D section for logistic constrain, a similar site setting emerges from all the surveys. The argillaceous cohesive and not liquefiable crust (CL, CH) can be estimated to be about 8–10 m thick from geotechnical tests and about 5–8 m thick from geophysical tests. These last tests evidence also a significant lateral variability of the crust thickness (higher in the NE portion of the 2D profile) with also relevant oscillations within the profile. In general, the proposed FC screening from the geophysical data appears to be satisfactory, with the great advantage with respect to the punctual geotechnical information of estimating the parameter variations along a wider portion of the site and therefore providing relevant information for the estimation of susceptibility to liquefaction. With respect to the geotechnical tests, the geophysical estimates report a less thick portion of the subsoil with FC > 80% and a less marked interface with the underlying sandy silt and silty sand with a FC transition and lateral variability. The geological setting emerging from the geophysical data appears to be coherent with respect to the presence at the site of widespread liquefaction phenomena. The combination of the geotechnical

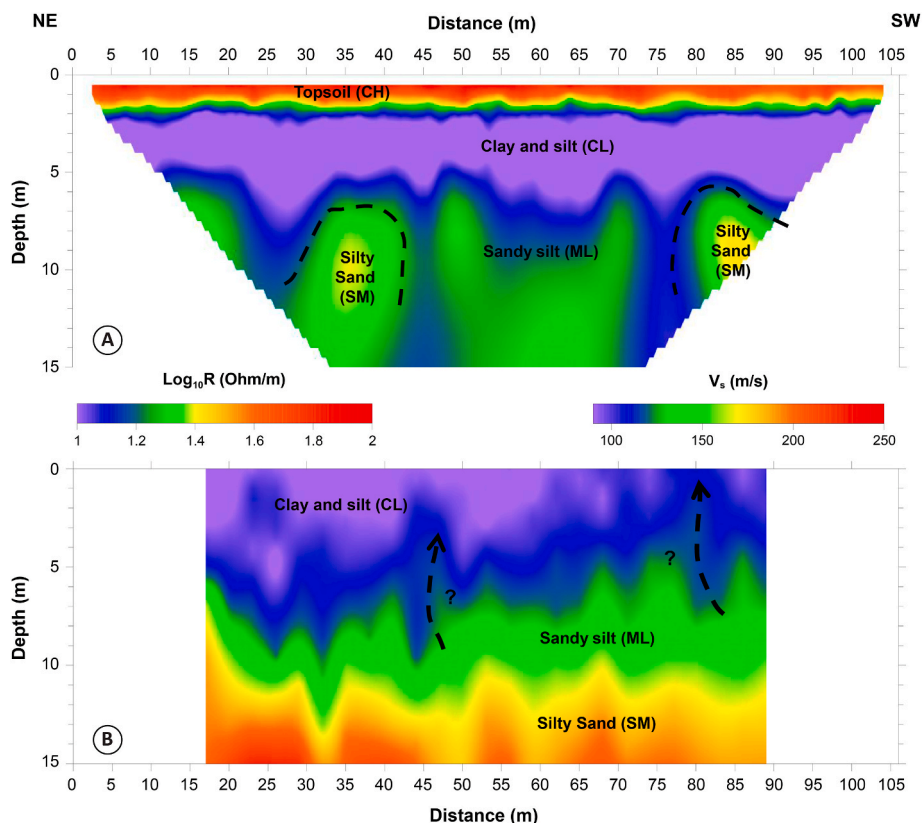


Fig. 7. Geophysical tests executed at the San Carlo test site (Fig. 1c) with superimposed stratigraphic interpretation: (a) ERT and (b) MASW2D.

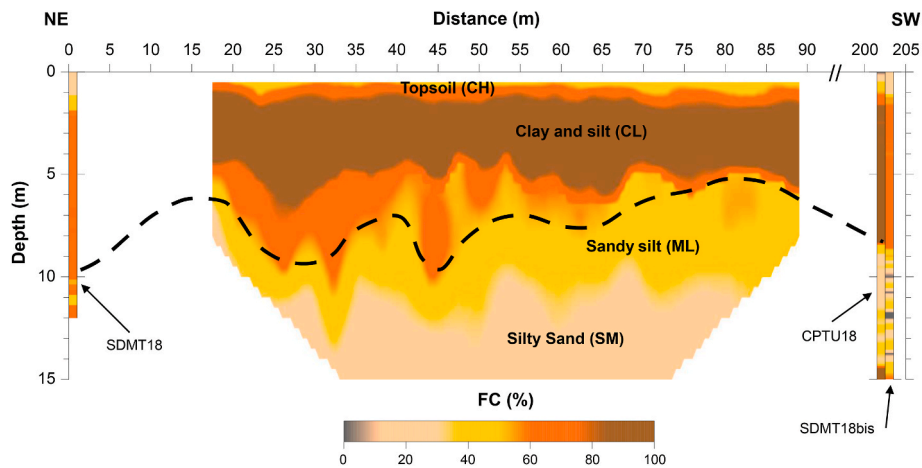


Fig. 8. Imaging of the FC from geotechnical and geophysical data at the San Carlo test site (Fig. 1c).

and geophysical tests has permitted to reconstruct the geometry and thickness of the fluvial channel sandy body that originated the liquefaction in 2012. This body appears oriented perpendicularly with respect to the 2012 liquefaction alignment and to the geophysical tests. The maximum thickness of the sandy body appears to be comprised between the 55 and 90 progressives, with a sharp lateral closure north-eastward in correspondence of the SDMT18 test (Fig. 6).

6. Conclusions

Specific fines content (FC) procedures, based on geotechnical and geophysical data, have been proposed for more proper liquefaction hazard estimations in the alluvial Emilia plain (Italy) affected by the 2012 seismic sequence. These methodologies are based on CPT or DMT or electrical resistivity and shear wave velocity measurements.

Specifically, a new and firstly proposed correlation between FC and DMT data has been developed and calibrated, increasing the potentiality of the DMT tests and its applicability in the study area. The paper shows the potentiality of the CPT and DMT cost-effective procedures in the definition of the FC vertical profile (1D imaging), supported by independent laboratory FC estimates at the calibration sites.

The linear geophysical surveys allowed to obtain 2D imaging of the fines content, able to distinguish the upper non-liquefiable high FC crust and the underlying lower FC sandy silt/silty sand layers. Moreover these techniques provided a reasonable subsoil reconstruction of alluvial succession, highlighting geometrical variability and grain-size. This approach, calibrated at the study sites, has provided relevant information for the estimation of liquefaction susceptibility along 2D profiles, and significant advantage with respect to the punctual estimation carried out by the geotechnical tests. The integration of punctual and linear investigations has also supported the reconstruction of the geometry and thickness of the 2012 liquefied deposits.

Funding

This work is partly funded by Search for Excellence – Uda 2019 (University of Chieti-Pescara, Italy), Evaluation and Improvement of Methods to Consider Influence of Surface Clay Layers on Liquefaction-Induced Settlement (CLIQUEST). However, the opinions, conclusions, and recommendations in this paper do not necessarily represent those of the sponsors.

Declaration of competing interest

The authors declare that they have no known competing financial interests or personal relationships that could have appeared to influence

the work reported in this paper.

Data availability

Data will be made available on request.

Acknowledgements

Special thanks to Studio Prof. Marchetti to freely provide the seismic dilatometer equipment for the field investigations, to Prof. Marco Stefani for the review of the manuscript and to Giacomo Maci to support the data collection. This work is partly funded by Search for Excellence – Uda 2019 (University of Chieti-Pescara, Italy), Evaluation and Improvement of Methods to Consider Influence of Surface Clay Layers on Liquefaction-Induced Settlement (CLIQUEST). However, the opinions, conclusions, and recommendations in this paper do not necessarily represent those of the sponsors.

References

- [1] Seed HB, Idriss IM. Simplified procedure for evaluating soil liquefaction potential. *J Soil Mech Found Div* 1971;97(9):1249–73.
- [2] Robertson PK, Wride CE. Evaluating cyclic liquefaction potential using the cone penetration test. *Can Geotech J* 1998;35(3):442–59.
- [3] Andrus RD, Stokoe II KH. Liquefaction resistance of soils from shear-wave velocity. *J Geotech Geoenviron Eng* 2000;126(11):1015–25.
- [4] Youd TL, Idriss IM, Andrus RD, Arango I, Castro G, Christian JT, Dory R, Finn WDL, Harder LF, Hynes ME, Ishihara K, Koester JP, Liao SSC, Marcuson WF, Martin GR, Mitchell JK, Moriwaki Y, Power MS, Robertson PK, Seed RB, Stokoe KH. Liquefaction resistance of soils: summary report from the 1996 NCEER and 1998 NCEER/NSF workshops on evaluation of liquefaction resistance of soils. *J Geotech Geoenviron Eng ASCE* 2001;127(10):817–33.
- [5] Idriss IM, Boulanger RW. Soil liquefaction during earthquakes. *Earthquake Engineering Research Institute*; 2008.
- [6] Kayen R, Moss RE, Thompson EM, Seed RB, Cetin KO, Der Kiureghian A, Tanaka Y, Tokimatsu K. Shear-wave velocity-based probabilistic and deterministic assessment of seismic soil liquefaction potential. *J Geotech Geoenviron Eng* 2013; 139(3):407.
- [7] Boulanger RW, Idriss IM. CPT and SPT based liquefaction triggering procedures. Report No. UCDC/GM.-14. 2014.
- [8] Marchetti S. Incorporating the stress history parameter KD of DMT into the liquefaction correlations in clean uncemented sands. *J Geotech Geoenviron Eng* 2016;142(2):04015072.
- [9] Rollins KM, Amoroso S, Andersen P, Tonni L, Wissmann KJ. Liquefaction mitigation of silty sands using rammed aggregate piers based on blast-induced liquefaction testing. *J Geotech Geoenviron Eng* 2021;147(9):04021085. [https://doi.org/10.1061/\(ASCE\)GT.1943-5606.0002563](https://doi.org/10.1061/(ASCE)GT.1943-5606.0002563).
- [10] Rollins KM, Roy J, Athanasopoulos-Zekkos A, Zekkos D, Amoroso S, Cao Z, Milana G, Vassallo M, Di Giulio G. A new VS-based liquefaction triggering procedure for gravelly soils. *J Geotech Geoenviron Eng* 2022;148(6):04022040. [https://doi.org/10.1061/\(ASCE\)GT.1943-5606.0002784](https://doi.org/10.1061/(ASCE)GT.1943-5606.0002784).
- [11] Amoroso S, García Martínez MF, Monaco P, Tonni L, Gottardi G, Rollins KM, Minarelli L, Marchetti D, Wissmann KJ. Comparative study of CPTU and SDMT in liquefaction-prone silty sands with ground improvement. *J Geotech Geoenviron*

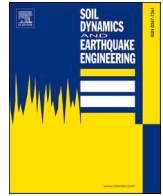
- Eng 2022;148(6):04022038. [https://doi.org/10.1061/\(ASCE\)GT.1943-5606.0002801](https://doi.org/10.1061/(ASCE)GT.1943-5606.0002801).
- [12] Suzuki Y, Koyamada K, Tokimatsu K. Prediction of liquefaction resistance based on CPT tip resistance and sleeve friction. In: Vol 1: proc, 14th international conference on soil mechanics and foundation engineering, hamburg, Germany; 1997. p. 603–6.
- [13] Maurer BW, Green RA, van Ballegooy S, Wotherspoon L. Development of region-specific soil behavior type index correlations for evaluating liquefaction hazard in Christchurch, New Zealand. *Soil Dynam Earthq Eng* 2019;117:96–105. <https://doi.org/10.1016/j.soildyn.2018.04.059>.
- [14] Bassal PC, Boulanger RW, DeJong JT. Site-specific CPT-based fines content correlations using percentile matching. In: *Geo-Congress 2022*:549–58. <https://doi.org/10.1061/9780784484043.053>.
- [15] Minarelli L, Amoroso S, Civico R, De Martini PM, Lugli S, Martelli L, Molisso F, Rollins KM, Salocchi A, Stefani M, Cultrera G, Milana G, Fontana D. Liquefied sites of the 2012 Emilia earthquake: a comprehensive database of the geological and geotechnical features (Quaternary alluvial Po plain, Italy). *Bull Earthq Eng* 2022: 1–39. <https://doi.org/10.1007/s10518-022-01338-7>.
- [16] Marchetti S, Crapps DK. *Flat dilatometer manual*. GPE incorporated; 1981.
- [17] Boncio P, Amoroso S, Vessia G, Francescone M, Nardone M, Monaco P, Famiiani D, Di Naccio D, Mercuri A, Manuel MR, Galadini F. Evaluation of liquefaction potential in an intermountain Quaternary lacustrine basin (Fucino basin, central Italy). *Bull Earthq Eng* 2018 Jan;16(1):91–111. <https://doi.org/10.1007/s10518-017-0201-z>.
- [18] Marchetti S, Monaco P, Totani G, Calabrese M. The flat dilatometer test (DMT) in soil investigations. A Report by the ISSMGE Committee TC16. In: Failmezger RA, Anderson JB, editors. *Proc, International conference on in situ measurement of soil properties and case Histories*, official version reprinted in *Flat dilatometer testing, Proc, 2nd international conference on the flat dilatometer*, vols. 7–48; 2001.
- [19] Passeri F, Comina C, Marangoni V, Foti S, Amoroso S. Geophysical monitoring of blast-induced liquefaction at the Mirabello (NE Italy) test site. *J Environ Eng Geophys* 2018;23(3):319–33. <https://doi.org/10.2113/JEEG23.3.319>.
- [20] Carcione JM, Ursin B, Nordskog JI. Cross-property relations between electrical conductivity and the seismic velocity of rocks. *Geophysics* 2007;72(5):E193–204.
- [21] Brovelli A, Cassiani G. A combination of the Hashin-Shtrikman bounds aimed at modelling electrical conductivity and permittivity of variably saturated porous media. *Geophys J Int* 2010;180(1):225–37.
- [22] Takahashi T, Aizawa T, Murata K, Nishio H, Consultants S, Matsuoka T. Soil permeability profiling on a river embankment using integrated geophysical data. In: *Proc, society of exploration geophysicists international exposition and 84th annual meeting SEG*; 2014. p. 4534–8.
- [23] Goff DS, Lorenzo JM, Hayashi K. Resistivity and shear wave velocity as a predictive tool of sediment type in coastal levee foundation soils. In: *Proc. 28th symposium on the application of geophysics to engineering and environmental problems SAGEEP*; 2015. p. 145–54.
- [24] Hayashi K, Inazaki T, Kitao K, Kita T. Statistical estimation of geotechnical soil parameters in terms of cross-plots of S-wave velocity and resistivity in Japanese levees. In: *2013 SEG Annual Meeting*; 2013. p. 1259–63.
- [25] Glover PW, Hole MJ, Pous J. A modified Archie's law for two conducting phases. *Earth Planet Sci Lett* 2000;180(3–4):369–83.
- [26] Vagnon F, Comina C, Arato A. Evaluation of different methods for deriving geotechnical parameters from electric and seismic streamer data. *Eng Geol* 2022; 303:106670.
- [27] Vagnon F, Comina C, Arato A, Chiappone A, Cosentini RM, Foti S. Geotechnical screening of linear earth structures: electric and seismic streamers data for hydraulic conductivity assessment of the Arignano earth dam. *J Geotech Geoenviron Eng* 2022;148(12).
- [28] Emergeo Working Group. Liquefaction phenomena associated with the Emilia earthquake sequence of may–june 2012 (northern Italy). *Nat Hazards Earth Syst Sci* 2013;13(4):935–47.
- [29] Ghielmi M, Minervini M, Nini C, Rogledi S, Rossi M. Late Miocene–Middle Pleistocene sequences in the Po Plain–Northern Adriatic Sea (Italy): the stratigraphic record of modification phases affecting a complex foreland basin. *Mar Petrol Geol* 2013;42:50–81.
- [30] Rovida A, Locati M, Camassi R, Lolli B, Gasperini P, Antonucci A. *Catálogo parametrico dei terremoti italiani (cpti15)*. Istituto Nazionale di Geofisica e Vulcanologia (INGV); 2016.
- [31] Bruno L, Amorosi A, Lugli S, Sammartino I, Fontana D. Trunk river and tributary interactions recorded in the Pleistocene–Holocene stratigraphy of the Po Plain (northern Italy). *Sedimentology* 2021;68(6):2918–43.
- [32] Stefani M, Minarelli L, Fontana A, Hajdas I. Regional deformation of late Quaternary fluvial sediments in the Apennines foreland basin (Emilia, Italy). *Int J Earth Sci* 2018;107(7):2433–47. <https://doi.org/10.1007/s00531-018-1606-x>.
- [33] Lugli S, Dori SM, Fontana D, Panini F. Composition of sands in cores along the high-speed rail (TAV): preliminary indications on the sedimentary evolution of the Modena plain 2004;17:379–89.
- [34] Fontana D, Amoroso S, Minarelli L, Stefani M. Sand liquefaction induced by a blast test: new insights on source layer and grain-size segregation mechanisms (Late Quaternary, Emilia, Italy). *J Sediment Res* 2019;89(1):13–27. <https://doi.org/10.2110/jsr.2019.1>.
- [35] ASTM D2487–11. *Standard practice for classification of soils for engineering purposes (unified soil classification system)*. West Conshohocken, PA: ASTM International; 2011.
- [36] Amoroso S, Milana G, Rollins KM, Comina C, Minarelli L, Manuel MR, Monaco P, Franceschini M, Anzidei M, Lusvardi C, Cantore L, Carpena A, Casadei S, Cinti FR, Civico R, Cox BR, De Martini PM, Di Giulio G, Di Naccio D, Di Stefano G, Facciorusso J, Famiiani D, Fiorelli F, Fontana D, Foti S, Madiati C, Marangoni V, Marchetti D, Marchetti SL, Martelli L, Mariotti M, Muscolino E, Pancaldi D, Pantosti D, Passeri F, Pesci A, Romeo G, Sapia V, Smedile A, Stefani M, Tarabusi G, Teza G, Vassallo M, Villani F. The first Italian blast-induced liquefaction test (Mirabello, Emilia-Romagna, Italy): description of the experiment and preliminary results. *Ann Geophys* 2017;60(5):S0556. <https://doi.org/10.4401/ag-7415>.
- [37] Amoroso S, Rollins KM, Andersen P, Gottardi G, Tonni L, García Martínez MF, Wissmann KJ, Minarelli L, Comina C, Fontana D, De Martini PM, Monaco P, Pesci A, Sapia V, Vassallo M, Anzidei M, Carpena A, Cinti F, Civico R, Coco I, Conforti D, Doumaz F, Giannattasio F, Di Giulio G, Foti S, Loddo F, Lugli S, Manuel MR, Marchetti D, Mariotti M, Materni V, Metcalfe B, Milana G, Pantosti D, Pesce A, Salocchi AC, Smedile A, Stefani M, Tarabusi G, Teza G. Blast-induced liquefaction in silty sands for full-scale testing of ground improvement methods: insights from a multidisciplinary study. *Eng Geol* 2020;265:105437. <https://doi.org/10.1016/j.enggeo.2019.105437>.
- [38] Suzuki Y, Sanematsu T, Tokimatsu K. Correlation between SPT and seismic CPT. In: *Geotechnical site characterization 1998*:1375–80.
- [39] Hashin Z, Shtrikman S. A variational approach to the theory of the elastic behaviour of multiphase materials. *J Mech Phys Solid* 1963 Mar 1;11(2):127–40.
- [40] Mavko G, Mukerji T, Dvorkin J. *The rock physics handbook: tools for seismic analysis of porous media*. Cambridge University Press Cambridge UK; 2009. <https://doi.org/10.1017/CBO9780511626753>.
- [41] ASTM D7400–14. *Standard test methods for downhole seismic testing*. ASTM International; 2014.
- [42] Butcher A, Campanella R, Kaynia A, Massarsch K. Seismic cone downhole procedure to measure shear wave velocity—A guideline prepared by ISSMGE TC10. In: *Geophysical testing in geotechnical engineering, proceedings of the XVIIth international conference on soil mechanics and geotechnical engineering, osaka, Japan*; 2005.
- [43] Loke MH, Barker RD. Rapid least-squares inversion of apparent resistivity pseudosections by a quasi-Newton method: geophysical Prospecting. <https://doi.org/10.1111/j.1365-2478.1996.tb00142.x>; 1996.
- [44] Amoroso S, Comina C, Marchetti D. Combined P- and S-wave measurements by seismic dilatometer test (SPDMT): a case history in Bondeno (Emilia Romagna, Italy). *Geotech Test J* 2020;43(2):383–93. <https://doi.org/10.1520/GTJ20180233>.
- [45] Comina C, Vagnon F, Arato A, Fantini F, Naldi M. A new electric streamer for the characterization of river embankments. *Eng Geol* 2020;276:105770. <https://doi.org/10.1016/j.enggeo.2020.105770>.
- [46] Comina C, Vagnon F, Arato A, Antonietti A. Effective vs and Vp characterization from Surface Waves streamer data along river embankments. *J Appl Geophys* 2020; 183:104221. <https://doi.org/10.1016/j.jappge.2020.104221>.
- [47] Anjom FK, Teodor D, Comina C, Brossier R, Virieux J, Socco LV. Full-waveform matching of VP and VS models from surface waves. *Geophys J Int* 2019;218(3): 1873–91.

Update

Soil Dynamics and Earthquake Engineering

Volume 173, Issue , October 2023, Page

DOI: <https://doi.org/10.1016/j.soildyn.2023.108156>



Corrigendum to “Fines content determination through geotechnical and geophysical tests for liquefaction assessment in the Emilia alluvial plain (Ferrara, Italy)” [Soil Dynam Earthq Eng 173 (2023) 108057–108068/ISSN 0267-7261]

Francesco Di Buccio^{a,*}, Cesare Comina^b, Daniela Fontana^c, Luca Minarelli^d, Federico Vagnon^e, Sara Amoroso^{a,d}

^a Dipartimento di Ingegneria e Geologia, Università degli Studi G. d'Annunzio di Chieti-Pescara, Pescara, Italy

^b Dipartimento di Scienze della Terra, Università degli Studi di Torino, Torino, Italy

^c Dipartimento di Scienze Chimiche e Geologiche, Università degli Studi di Modena e Reggio Emilia, Modena, Italy

^d Istituto Nazionale di Geofisica and Vulcanologia, Sezione Roma1, L'Aquila, Italy

^e Dipartimento di Ingegneria dell'Ambiente, del Territorio e delle Infrastrutture, Politecnico di Torino, Torino, Italy

The authors regret to inform of an error in the paper that requires the replacement of Fig. 5. The error concerns Fig. 5c, in which the represented equation does not correspond to the correct one given in the body

of the paper. The correct equation is now reported in the figure below and in the attached file.

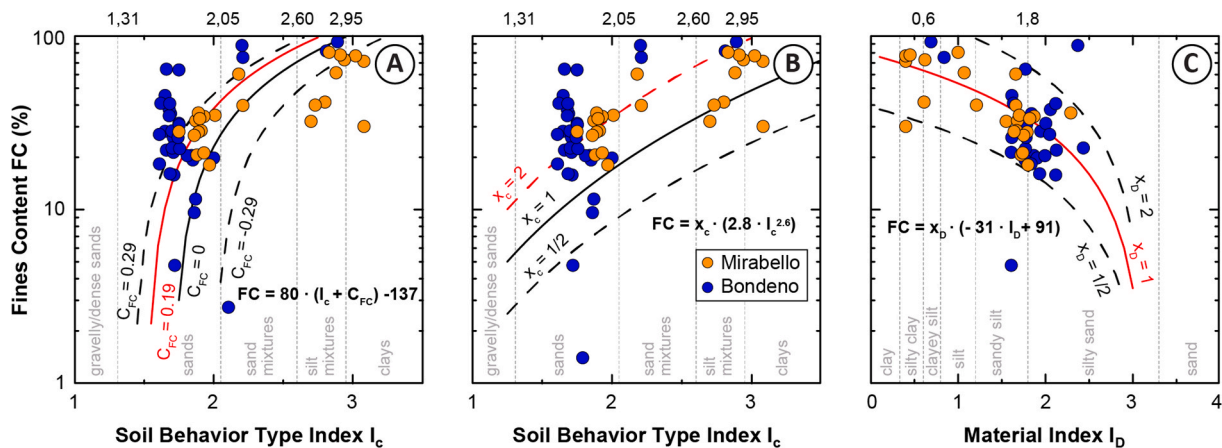


Fig. 5. FC estimates using in-situ tests at the Mirabello and Bondeno test sites: (a) calibration of the I_c -FC chart by [7]; (b) calibration of the I_c -FC chart by [38]; (c) I_D -FC chart proposed in this study based on DMT data.

The authors would like to apologise for any inconvenience caused.

DOI of original article: <https://doi.org/10.1016/j.soildyn.2023.108057>.

* Corresponding author. University of Chieti-Pescara, Italy.

E-mail address: francesco.dibuccio@unich.it (F. Di Buccio).

<https://doi.org/10.1016/j.soildyn.2023.108156>

Available online 31 July 2023

0267-7261/© 2023 Elsevier Ltd. All rights reserved.